Published in final edited form as:
Neurochem Int. 2008 May ; 52(6): 1176–1187. doi:10.1016/j.neuint.2007.12.008.

Protective effects of tetramethylpyrazine on rat retinal cell cultures

Zhikuan Yang[a], **Qingjiong Zhang**[a], **Jian Ge**[a,*], and **Zhiqun Tan**[b,*]

a*State Key Laboratory of Ophthalmology, Zhongshan Ophthalmic Center, Sun Yat-sen University, Guangzhou 510060, China*

b*Department of Neurology and Institute of Brain Aging and Dementia, University of California Irvine School of Medicine, Irvine, CA 92697, USA*

Abstract

The retinal degeneration characterized with death of retinal ganglion cells is a pathological hallmark and the final common pathway of various optic neuropathies. Thus, there is an urgent need for identifying potential therapeutic compounds for retinal protection. Tetramethylpyrazine has been suggested to be neuroprotective for central neurons by acting as an antioxidant and a calcium antagonist. In this study, we tested the effects of tetramethylpyrazine on the viability of both neuronal and non-neuronal cells in mixed rat retinal cell cultures during a long-term cultivation or following hydrogen peroxide treatments. Cellular and biochemical analyses demonstrated that 50 μM tetramethylpyrazine significantly preserved neuronal morphology and survival in retinal cell cultures following 4-week in vitro cultivation as well as lethal exposures to hydrogen peroxide (10μM or 50 μM for 24 hr). Hydrogen peroxide treatments induced remarkable increases in lipid peroxidation and mitochondrial ROS generation paralleled by the loss of mitochondrial membrane potential, microtubule-associated protein-2 (MAP-2) in neuronal soma and rattin peptide in cultured cells. Addition of tetramethylpyrazine in the cultures efficiently attenuated the signs of oxidative stress and retained abundance of MAP-2 and rattin in association with cell survival. In addition, siRNA-mediated downregulation of MAP-2 or rattin significantly increased the vulnerability of retinal neurons or the number of degenerating cells in the cultures, respectively, whereas exogenous humanin peptide, an analog of rattin, promoted cell survival in cultures under hydrogen peroxide attacks. These results suggest that tetramethylpyrazine protect retinal cells through multiple pathways and might be a potential therapeutic candidate for retinal protection in certain optic neuropathies.

Keywords

Neuroprotection; Tetramethylpyrazine; Retinal cell culture; Oxidative stress; Cell death

*Corresponding authors: **Zhiqun Tan, M.D., Ph.D.** Department of Neurology, University of California Irvine School of Medicine, 100 Irvine Hall, ZOT 4275, Irvine, CA 92697-4275, Tel: 949-824-1669; Fax: 949-824-2436, Email: tanz@uci.edu, **Jian Ge, M.D., Ph.D.** Professor & Director, Zhongshan Ophthalmic Center, Sun Yat-sen University, 54 Xianlie Road, Guangzhou 510060, China, Email: gejian@mail.sysu.edu.cn

Introduction

The death of retinal ganglion cells (RGC) is a pathological hallmark as well as the final common pathway of various optic neuropathies, such as glaucoma, ischemia and aging-related retinal degeneration (Levin, 1997; Farkas and Grosskreutz, 2001). Although the molecular mechanism of retinal degeneration remains poorly understood, accumulating evidence suggests that oxidative stress, excitotxocity, and coherent intracellular calcium and proteasomal dysregulation, mitochondrial dysfunction and/or endoplasmic reticulum stress might have been profoundly implicated in the pathogenesis of retinal cell death (Bahr, 2000; Farkas and Grosskreutz, 2001). In this regard, excessive exposure of RGC to excitory amino acid glutamate causes apoptotic cell death in cultured RGC (Ferreira et al., 1998; Li et al., 1999). This excitotoxic mechanism has been thought in association with RGC loss in glaucoma and retinal ischemia as well (Kapin et al., 1999; Luo et al., 2001; Guo et al., 2006). Increased reactive oxygen species (ROS) with reduced antioxidant activity are always linked with degenerating changes in retina under neurologic insults (Beatty et al., 2000; Cai et al., 2000; Tezel, 2006). ROS-induced oxidative damage, such as lipid peroxidation and protein carbonylation, has been repetitively demonstrated in various neurodegenerative disorders including retinopathies. Accordingly, antioxidants have been extensively investigated as potential pharmacological therapies for neuronal degeneration including optic neuropathies (Richer, 2000; Barnham et al., 2004; Casetta et al., 2005).

Tetramethylpyrazine (TMP), an active ingredient in and an extract from a Chinese herbal medicine, *Ligusticum wallichi* Franchat *(chuanxiong)*, has been commonly used in the clinic for treatment of cardiovascular diseases in China (Ge and Zhang, 1994; Xu et al., 2003). Previous studies have demonstrated strong neuroprotective effects of TMP both in vitro and in vivo. In this regard, TMP significantly suppresses oxidative stress and attenuates neuronal cell death in neuronal cultures induced by the excitotoxicity of glutamate analog (Li et al., 2000; Shih et al., 2002; Liao et al., 2004) and iron-mediated oxidative damage (Zhang et al., 2003). TMP is also demonstrated as a calcium antagonist (Pang et al., 1996). Systemic administration of TMP protected neuronal cells against ischemic or traumatic brain or spinal cord injury and promoted functional recovery in rodents and rabbit (Fan et al., 2006; Kao et al., 2006). Improvements of learning and cognitive function by TMP were also reported in rodents following D-galactose- or arterial occlusion-induced brain lesions (Ni et al., 1995; Zhang et al., 2004). In addition, TMP protects photoreceptor from drug-induced damage as well as optic nerve axon lesions caused by intraocular hypertension (Li et al., 2000; Yang et al., 2005). Despite accumulating reports showing the cytoprotective effects of TMP, the pharmacological mechanism of TMP for neuroprotection is still poorly understood at the molecular level.

At subcellular and molecular levels, as both targets and main sources of endogenous ROS mitochondria have been considered as the central players for the signal transduction of cell death through releasing a group of apoptogenic proteins such as cytochrome c into cytosol following a collapse of their membrane integrity (Parone et al., 2003; Lin and Beal, 2006). In this regard, Bcl-2 family members are the central regulators for the mitochondrial membrane permeability (Kroemer and Reed, 2000). Among a long list of Bcl-2 interacting molecules, humanin as well as its homolog, i.e., rattin, is recently identified as a small antiapoptotic peptide in human and rodent cells, respectively (Hashimoto et al., 2001; Caricasole et al., 2002). Through interacting with Bid to inhibit Bax protein activity, humanin has been found to protect neuronal cells from a variety of toxic insults (Guo et al., 2003; Nishimoto et al., 2004). However, whether humanin/rattin plays a role in modulation of mitochondrial function and whether it is affected by the intervention of TMP in retinal cells in response to oxidative insults are completely unknown. In the present study, we demonstrated TMP-mediated protection for both neurons and non-neuronal cells in the mixed retinal cell cultures following a long-term

cultivation as well as lethal exposures to hydrogen peroxide (H_2O_2). While examining the molecular effects of TMP on retinal cells, we found that, in addition to its antioxidant potentialities, TMP retained abundance of MAP-2, a key regulator for microtubule structures as well as a receptor for growth and environmental factors in neurons (Dehmelt and Halpain, 2005; Fontaine-Lenoir et al., 2006). As downregulation of MAP-2 significantly increased vulnerability to insults, preservation of MAP-2 protein by TMP was associated with neuronal survival. Interestingly, we also observed the similar effects of TMP on expression of rattin correlated with cell survival in cells under stresses. These findings suggest that TMP confer multifold protection for retinal cells and might therefore be a potential therapeutic candidate for retinal protection in certain retinopathies.

Materials and Methods

Materials

Poly-L-lysine (MW = 70-150 kDa), purified TMP, 30% hydrogen peroxide (H_2O_2), total protein assay kit, rabbit anti-glial fibrillary acidic protein (GFAP) polyclonal IgG, rabbit anti-rattin polyclonal IgG, FITC-conjugated goat anti-rabbit IgG, and Cy3-conjugated sheep anti-mouse IgG were purchased from Sigma-Aldrich (St. Louis, MO). Cy3-conjugated donkey anti-rabbit IgG was purchased from Chemicon (Temecula, CA). Live-dead cell assay kit was obtained from Biovision (Exton, PA). Mouse anti-MAP-2 monoclonal IgG was obtained from Covance (Denver, PA). In situ cell death detection kit/fluorescein or TMR red was purchased from Roche (Indianapolis, IN). BIOXYTECH® MDA-586™ assay kit was from Oxis International (Portland, OR). Amersham ECL Reagents for Western blotting were obtained from GE Healthcare Bio-Sciences (Piscataway, NJ). Tetramethylrhodamine methyl ester (TMRM), Hoechst 33342, MitoSOX Red, Lipofectamine 2000 and all the cell culture media/reagents and salt solutions were obtained from Invitrogen (Invitrogen, Carlsbad, CA). VectaShield mounting medium was purchased from Vector Laboratories (Burlingame, CA). ImProm-II™ reverse transcription system and reagents for polymerase chain reaction (PCR) were purchased from Promega (Madison, WI). Silencer siRNA Construction kit was obtained from Ambion (Houston, TX). Control siRNA was purchased from Santa Cruz Biotechnology (Santa Cruz, CA). Green fluorescent protein (GFP) vector, pEGFP-C3, was purchased from Clontech (Mountain View, CA). Humanin peptide was purchased from American Peptide (Sunnyvale, CA). All of the DNA oligonucleotides used for both PCR and siRNA construction were synthesized by Integrated DNA Technologies (Coralville, IA). Unless otherwise noted, all other chemicals were purchased from Sigma-Aldrich.

Animals and preparation of mixed retinal cell cultures

Sprague-Dawley (SD) rat pups (postnatal day 5~6) were sacrificed under CO_2-gas-induced anesthesia, and the eyes were immediately enucleated. The retinas were dissected in Ca^{2+}/Mg^{2+}-free Hank's balanced salt solution by carefully removing the anterior segments under stereoscope. Dissected retinas were then incubated in 0.2% trypsin at 37 °C for 5 min, triturated, plated onto poly-L-lysine-coated culture dishes or 4-well chamberslides at a density of 10^4/cm^2 in Neurobasal medium supplemented with B27 and GlutaMAX (Invitrogen), and grown in a humidified atmosphere containing 5% CO_2 at 37 °C. Media were changed every other day during the entire experimentation period. All experiments were performed in accordance with the guidelines regarding animal research issued by the National Institutes of Health as well as the Institutional Animal Care and Use Committees.

Treatments of retinal cell cultures

TMP was prepared as a 50 mM stock in dimethylsulfoxide (DMSO):saline (1:1, v/v). In the experiments to test the effects of TMP on cell survival following 4-week cultivation, 50 μM TMP or equal volume of vehicle was included in Neurobasal/B27 culture media from the third

day after cell plating. H_2O_2 was prepared by dilutions with culture media from a 30% stock. For H_2O_2-induced cytotoxicity and TMP-mediated neuroprotection experiments, the indicated amounts of drugs or equal volumes of vehicles were directly added to the culture media of cells one week after plating. These dosages were determined by preliminary experiments at the beginning. To test the neuroprotective effects of humanin peptide, 10 μM humanin or an equal volume of vehicle was directly included in the Neurobasal/B27 media 2 hr before H_2O_2 treatments. After treatments, cells were directly assayed for cell viability, harvested for biochemical analyses, or fixed for immunocytochemistry.

siRNA preparation and transfections

siRNAs were prepared using the Ambion's Silencer siRNA Construction Kit according to the manufacturer's protocol. siRNA corresponding to rat MAP-2 siRNA1 sequence as previously described (Krichevsky and Kosik, 2002) was synthesized using the following oligonucleotide templates: sense 5′-CGAGAGGAAAGACGAAGGATTCCTGTCTC-3′ and antisense 3′-TCCTTCGTCTTTCCTCTCGTG CCTGTCTC -5′. The templates used for synthesis of siRNA against rattin were sense 3′-AACGAGGGTTCAACTGTCTCTCCTGTCTC-5′ and antisense 3′-AAAGAGACAGTTGAACCCTCGCCTGTCTC-5′. Transfections of siRNA were performed with Lipofactamine 2000 in both 6-well plates and 2-chamber slides as described previously (Tan et al., 2007). Briefly, each 4 μl Lipofactamine diluted in 100 μl Opti-MEM was mixed with 100 pmol MAP-2 siRNA or 100 pmol rattin siRNA plus 2 μg pEGFP-C3 plasmid in 100 μl Opti-MEM and formulated at room temperature for 20 min. Per well, 200 μl of formulated Lipofactmaine-siRNA mixture was directly applied in the final volume of 2 ml Neurobasal/B27 media for 6-well plates and 40 μl mixture was added into 0.5 ml media for 2-chamber slides. The media were changed with fresh Neurobasal/B27 for further cultivation or treatments with TMP and/or H_2O_2 16 hr after transfections. Cells transfected with a control siRNA purchased from Santa Cruz Biotechnology were used as controls.

Morphology

After treatments, the general morphology of mixed retinal cell cultures was directly examined by differential interference contrast (DIC) microscopy with a Leica DM IRB microscope at a magnification of 200x. Images were recorded using a Spot II CCD camera.

Live-dead cell assay

24 hr after H_2O_2 and/or TMP treatments, the cells were directly stained with Live-dead cell staining kit according to the manufacturer's protocol. The results were evaluated by fluorescence microscopy with a Leica DM IRB microscope. Images were recorded using a Spot II CCD camera with equal exposure times for all the different treatments. For quantification, all green- (live) or red- (dead) fluorescent cells were counted in 6 randomly chosen, non-overlapped fields at a magnification of 200x.

Mitochondrial membrane potential assay

Cells were loaded with 20 nM mitochondrial membrane-potential-sensitive dye TMRM and 10 nM Hoechst 33342 in Neurobasal medium for 15 min in 37 °C and 5% CO_2 after specific treatments. Digital imaging of TMRM/Hoechst 33342-stained cells was performed in the same way for live-dead cell assay.

TdT-mediated dUTP nick end-labeling (TUNEL)

After treatments, the retinal cells grown on chamberslides were fixed with 4% paraformaldehyde (PFA) in 1 × PBS (pH 7.4) at 4 °C for 20 min or 95% methanol at 4 °C for 10 min (for GFP-transfected cells) as described in our previous work (Tan et al., 2001). TUNEL was performed following fixation using an In Situ Cell Death Detection (fluorescein or TMR

red) kit according to the manufacturer's protocol. For double-labeling slides were incubated in blocking buffer for 30 min at room temperature after TUNEL staining and followed by staining with a mouse anti-MAP-2 or a rabbit anti-rattin IgG. The immunoreactivity of MAP-2 or rattin was detected using a Cy3-conjugated sheep anti-mouse or donkey anti-rabbit IgG and fluorescence microscopy.

Immunocytochemistry

Following either PFA or methanol fixation, cells were then incubated with a mouse anti-MAP-2 IgG (1:500 in 1×PBS) or a rabbit anti-rattin IgG (1:200 in 1×PBS) alone or a mouse anti-MAP-2 IgG (1:500 in 1×PBS) with either a rabbit anti-rattin IgG or a rabbit anti-GFAP IgG (1:400 in 1 ×PBS) at room temperature for 3 hr after 30 min blocking with a buffer containing 20 mM L-lysine and 3% rabbit and goat sera in 1×PBS at room temperature. The immunoreactivity of MAP-2, GFAP and rattin was visualized with fluorescence microscopy following staining with Cy3-conjugated either sheep anti-mouse or donkey anti-rabbit IgG, or FITC-conjugated goat anti-rabbit IgG and covered with VectaShield 4′,6′-diamidino-2-phenylindole (DAPI)-containing mounting medium. For quantification, all MAP-2-, GFAP- and/or TUNEL-positive cells following immunocytochemistry were counted in 10 randomly chosen and non-overlapped fields at magnification of 200x. In rattin siRNA/GFP transfected cells, TUNEL-positive cells were counted from 100 randomly chosen GFP-positive cells.

Western blotting

Retinal cell cultures were harvested at indicated times and sonicated in lysis buffer containing 50 mM Tris-HCl (pH 7.5), 5 mM EDTA, 150 mM NaCl, 0.5% NP-40 plus protease inhibitor cocktail mixture following specific cultivation or treatments. The resultant cell lysates were examined for total protein concentrations using Sigma total protein assay kit and 20~40 μg total protein of each lysate were resolved by 8% or 12.5% sodium dodecyl sulfate-polyacylamide gel electrophoresis (SDS-PAGE) and transferred to a nitrocellulose membrane overnight at 4 °C. The membranes were incubated in Blotto blocking buffer for 45 min followed by incubation with a primary antibody for 3 hr and a horseradish peroxidase-conjugated secondary antibody for 30 min. The results were visualized by ECL enhanced chemilluminescence kit. Quantification of gel pixel intensity was performed with the UN-Scan-It software.

Synthesis of cDNA and PCR analysis

Total RNA was prepared from retinal cell cultures at indicated times after treatments using TRIZOL (Invitrogen). Total RNA (1.5 μg) was reverse transcribed with 1 μg oligo(dT) in 20 μl reaction mixture provided by ImProm-II™ reverse transcription system following the manufacturer's instruction. The reaction was stopped by adding 100 μl 10 mM Tris-HCl (pH 7.4) and 1 mM EDTA. 5 μl of the final diluted cDNA mixture was used for each PCR reaction. To analyze expression of rattin transcripts, PCR was performed using sense primer 5′-TTAGGGACTAGAATGAATGG-3′ and anti-sense primer 5′-GGAGCTTCAATTTACTAGTT-3′ based on published studies (Caricasole et al., 2002). PCR reactions were subjected to 30 cycles (94 °C × 30 sec, 55 °C × 30 sec, 72 °C × 30 sec) in a Perkin Elmer DNA Thermal Cycler and PCR products were resolved by 1.5% agarose gel electrophoresis. β-actin was amplified as cDNA loading controls using the same condition except that primers were 5′-ATCAACTGGAGAACCATG CCCTGA-3′ (sense) and 5′-AACGGCACTAGAAGAAGCTG GGAA-3′ (antisense). Quantification of gel pixel intensity was performed in the same way for Western blotting with the UN-Scan-It software.

Determination of lipid peroxidation and mitochondrial ROS

Lipid peroxidation was examined through measuring malondialdehyde (MDA) content using a BIOXYTECH® MDA-586™ assay kit following manufacturer's protocol with minor modification. Briefly, cells were harvested and homogenized in 0.1M phosphate buffer (pH7.4) and centrifuged at 14000 rpm at 4C for 30 min. Protein concentrations of the supernatants were determined using Total Protein Assay Kit and immediately stored at -80 °C for use. To assay MDA content in the lysates (supernatants) prepared, 75μg total protein of lysate (50 μl) was incubated with 2.5 μl probucol, 160 μl diluted R1 reagent and 37.5 μl of R2 at 45 °C for 60 min. The reaction mixture was then centrifuged at 10,000 × g for 10 min and OD of the supernatant was detected at 586 nm using a Beckman Spectrophotometer. MDA concentrations were calculated based on tetramethoxypropane (TMOP) standard curve as described in the manufacturer's protocol.

Mitochondrial ROS in cells following treatments was detected by MitoSOX Red mitochondrial superoxide indictor dye following the manufacturer's protocol. Briefly, 5μM MitoSOX Red was directly included in the Neurobasal/B27 cell growth media for 10 min at 37 °C with 5% CO2. Mitochondrial superoxides were visualized in situ under fluorescence microscopy following wash with warm PBS.

Data analysis

In all the graphs that include error bars, the data points represent the means ± S.E.M. from 3~5 independent repeats (i.e., N = 3~5). Where applicable multiple comparisons were performed by one-way ANOVA followed by Student *t*-test in Microsoft Excel software. The differences between groups were considered statistically significant when P values ≤ 0.05.

Results

TMP prolonged retinal cell survival in long-term cultivation in vitro

Due to the high vulnerability of differentiated neurons to the disturbance in the ambient environment, viable primary neuronal cultures show gradual cell death 2 or 3 weeks after plating. Initially-mixed embryonic or postnatal neural cultures growing in serum-free Neurobasal/B27 media will be dominated by differentiated neurons as a result of glial loss during the cultivation (Brewer et al., 1993). As previous studies showed protective effects of TMP on both cerebral and spinal neurons (Shih et al., 2002; Fan et al., 2006), we firstly examined whether TMP would promote survival of retinal cell cultures by assessing the effect of TMP on the viability of retinal cells following 4-week cultivation in vitro. Accordingly, 50 μM TMP or vehicle was included in Neurobasal/B27 growth media during the cultivation. Notably, DIC microscopy revealed a healthy appearance of retinal neurons with plumpy neuronal processes that were lined by non-neuronal-looking cells underneath in TMP-treated cultures 4 weeks after plating (Fig. 1B). In contrast, the cultures with vehicle manifested relatively low numbers of cells in the field and an unhealthy appearance of retinal neurons with retraction of processes and shrinkage of cell bodies (Fig. 1A). Dual immunocytochemistry of both MAP-2 and GFAP, two molecular markers for neurons and astrocytes, respectively, revealed MAP-2-positive neurons (Figs. 1C-F) underlined by the confluent astrocytic glia (Figs. 1G-H) in both vehicle- and TMP-treated cultures. Quantification of these results demonstrated significantly higher numbers of MAP-2-positive retinal neurons (Fig. 1I) and a slight increase, which is not statistically significant, in the number of astrocytes in the TMP-treated cultures than these with vehicle (Fig. 1J).

TMP attenuated hydrogen peroxide-induced cell death in retinal cell cultures

Accumulating evidence suggests that the cytoprotective effect of TMP might be mediated by its antioxidant potentialities in cells (Shih et al., 2002; Zhang et al., 2003; Yang et al., 2005). In agreement with these observations, we detected a strong protective effect of TMP on retinal cells against ROS generator, H_2O_2, -induced cytotoxicity. One-week old retinal cell cultures were treated with low (10 μM) or high (50 μM) H_2O_2 with either 50 μM TMP or vehicle. 24 hr after treatments cultures were directly assayed by Live-dead cell assay kit. Fluorescence microscopy demonstrated massive cell death following either low or high dose of H_2O_2 treatment (Figs. 2A-F). In contrast, in the presence of 50 μM TMP most cells were stained as green for "live" following H_2O_2 treatments (Figs. 2J-O). Quantification of these results shows that TMP significantly protected culture cells from H_2O_2-induced cell death (Fig. 2P).

Inhibition of H_2O_2-induced neuronal cell death was further confirmed by double labeling of TUNEL and MAP-2 neuronal marker. Strikingly, following H_2O_2 treatments most cells were TUNEL-negative in the presence of TMP (Fig. 3A), while these in vehicle groups exhibited extensively TUNEL-positive (Fig. 3D). Merged images of MAP-2-immunoreactivity and TUNEL signal demonstrated massive neuronal cell damage in the "H_2O_2+vehicle"-treated cells, but very little in the "H_2O_2+TMP"-treated cells. Quantifications of TUNEL-positive cells relative to the total number of cells based on DAPI-counterstained nuclei (Fig. 3G) or (MAP2 +TUNEL)-positive cells relative to MAP-2-positive neurons only (Fig. 3H) demonstrated significantly lower numbers of TUNEL-positive cells for the H_2O_2-treated cultures in the presence of TMP than those with the vehicle, suggesting a significant protection of TMP on both neuronal and non-neuronal cells in mixed retinal cell cultures against H_2O_2-induced cell damage.

Attenuation of mitochondrial membrane depolarization and oxidative stress by TMP

As known, mitochondrial collapse is a common and essential step in cell death pathways. Therefore, we sought to examine whether TMP prevents depolarization of mitochondrial membrane during the neuronal cell death induced by H_2O_2 treatments. The loss of mitochondrial membrane potential was evaluated by TMRM staining. Consistent with the results from cell death assays, TMRM was observed to stain almost all the cells in control (Figs. 4A & B) and most H_2O_2-treated cells with the addition of TMP (Figs. 4E & F), but not in these cultures with H_2O_2 and vehicle (Figs. 4C & D). These results indicate that TMP attenuates H_2O_2-induced loss of mitochondrial membrane potential, i.e., depolarization. Interestingly, the loss of mitochondrial membrane potential in retinal cells following H_2O_2 treatments correlated with a remarkable accumulation of mitochondrial ROS (Fig. 4H) in comparison with either vehicle controls (Fig. 4G) or those with TMP (Fig. 4I) as detected by MitoSOX Red staining. To examine this further the products of lipid peroxidation, MDA, in whole cell lysates were measured. 24 hr treatment with either 10 or 50 μM H_2O_2 resulted in a striking elevation of MDA amounts in association with increased retinal cell death (Fig. 4J). In contrast, this increase was significantly inhibited by the addition of TMP (Fig. 4J).

TMP retained neuronal MAP-2 to contribute to the protection of retinal neurons

When labeling retinal neurons with MAP-2 antibody as shown above, we detected the cytoplasmic immunoreactivity of MAP-2 present in both neuronal soma and processes in normal retinal neurons in 1~2-week old untreated cultures (data not shown) as well as those with the presence of TMP in their growth media (Figs. 1D, F&H; Figs. 3B&C). Interestingly, we noticed a remarkable loss of MAP-2 immunoreactivity in the compartment of cell soma following either long-term cultivation or treatments with H_2O_2 (Figs. 1C, E & G; Figs. 3E &F). These findings were corroborated at protein level by Western blot using the same MAP-2 antibody (Fig. 5A, first panel). To investigate the significance of MAP-2 downregulation in cell soma of neurons under challenging, specific siRNA against rat MAP-2 was employed to

knockdown expression of MAP-2 protein. 16 hr after transfection with MAP-2 siRNA cells exhibited a progressive decrease in levels of MAP-2 up to 40 hr as shown by Western blots (Fig. 5A, 3rd panel). Apparently, the loss of MAP-2 in cell soma seems neither to cause significantly visible morphological changes nor directly to trigger neuronal cell death in our experimentation periods as examined by double labeling of TUNEL and MAP-2 (Fig. 5B). Since MAP-2 regulates the structure and function of microtubule system (Dehmelt and Halpain, 2004), we hypothesized that loss of MAP-2 in neuronal soma might raise the vulnerability of neurons in response to oxidative stress. To test this premise, cells were treated with a sublethal dose of 0.5 μM H_2O_2 for 24 hr at 16 hr after siRNA transfection. Under this circumstance, there were no noticeable cell death in both untransfected (data not shown) or control siRNA-transfected retinal cells as detected by TUNEL (Fig. 5D). In contrast, most neurons whose soma regions showed very low levels of MAP-2 immunoreactivity due to siRNA transfection were TUNEL-positive following exposures to the low level (0.5 μM) of H_2O_2 (Fig. 5C). Quantification of the results revealed a statistically significant increase in the number of TUNEL-positive neurons following siRNA-mediated MAP-2 downregulation (Fig. 5E).

TMP inhibited ROS-induced downregulation of rattin associated with retinal cell survival

Previous studies found that TMP protected mitochondrial function through regulating expressions of mitochondrial Bcl2 family proteins that directly modulate mitochondrial permeability in the central nervous system (CNS) (Cheng et al., 2006; Kao et al., 2006). Since the mitochondrial integrity is modulated by humanin/rattin, we sought to examine whether TMP also modulates expression of rattin in retinal cells to contribute to its neuroprotective effects. Double labeling of rattin and MAP-2 detected a dramatic loss of rattin immunoreactivity in cells after 10 μM H_2O_2 treatment (Figs. 6C&D). Conversely, the control and those with TMP showed evident immunoreactive signals for most cells (Figs. 6A, B, E &F). These results were further strengthened at the protein level by Western blot and at the mRNA level by RT-PCR analysis of rattin transcripts (Figs. 6G&H). Similar loss of rattin protein was also detected in cells after 4-week long-term cultivation. To investigate the pathophysiological significance of rattin loss in the pathogenesis of retinal cell death, a specific siRNA targeting rattin mRNA was used to knockdown expression of rattin in cultured retinal cells. siRNA-mediated downregulation of rattin protein was firstly confirmed by both immunocytochemistry (Figs. 6L-N) and Western blots (Fig. 6U) 30 hr after transfection. Control siRNA had no effect on abundance of rattin protein (Figs. 6I-K, U). TUNEL staining detected that most rattin siRNA-transfected cells as manifested by GFP fluorescence were TUNEL-positive, whereas control siRNA showed no effect on TUNEL signal. Quantification of these results demonstrated a striking increase in cell damage as shown by TUNEL following downregulation of rattin. To evaluate further the importance of rattin in retinal cell survival, we investigated whether addition of exogenous rattin analog/homolog peptide, i.e., humanin, protects retinal cells from H_2O_2-induced cell death. Fluorescence microscopy following Live-dead cell assay after treatments demonstrated that the majority of cells in H_2O_2-treated cultures were stained as “live” in the presence of 10 μM humanin. In contrast, most cells with vehicle showed dead following the identical H_2O_2 treatments (Figs. 6I-O).

Discussion

The beneficial effects of TMP on the CNS against stresses have previously been demonstrated (Liao et al., 2004; Kao et al., 2006). TMP significantly attenuates neural cell damage in the CNS in response to either toxic or traumatic insults and shows strong anti-oxidant activity (Shih et al., 2002; Liao et al., 2004). Here, we demonstrate that TMP prolonged neuronal cell survival and rescued cells from H_2O_2-induced degeneration in mixed retinal cell cultures. TMP maintained a significantly higher number of MAP-2-positive neurons in the mixed retinal cell

cultures after 4-week cultivation. Similar protective effects were also observed for both MAP-2-labeled neurons and non-neuronal cells, of which the majority of them were identified as GFAP-positive astrocytes, in cultures following H_2O_2 exposures. Importantly, these results were correlated with the striking inhibition of both lipid peroxidation and mitochondrial ROS production in the cultures with TMP. Our findings therefore substantiate the knowledge about the antioxidant potency of TMP for neural cells.

The pharmacological significance of TMP-mediated preservation of MAP-2 protein in neurons is underscored by the detection of an increased vulnerability of cells with low level of MAP-2 to insults in this study. siRNA-mediated suppression of MAP-2 dramatically raised the degree of damage for neurons following sublethal H_2O_2 exposures. Besides acting as an important regulator for the cytoskeleton through the interaction with microtubules, MAP-2 protein has been known to play key roles in neuronal responses to growth factors and other environmental factors (Dehmelt and Halpain, 2005; Fontaine-Lenoir et al., 2006). Loss of MAP-2 could be a severe disturbance in the dynamic integrity of neuroarchitechure and the metabolic homeostasis of neurons and thereby promote neuronal cell death in response to stress. Accordingly, specific siRNA-mediated downregulation of MAP-2 dramatically increased vulnerability of retinal neurons to ROS attacks. In this case, about 70% of retinal neurons that had very low levels of MAP-2 following siRNA transfection were detected as TUNEL-positive due to a sublethal exposure to ROS. This observation is in agreement with previous studies that demonstrated reduction of MAP-2 in degenerating neurons induced by ROS-generating agents in vitro or ischemia in vivo (Wang et al., 2001; Fifre et al., 2006). Although the discrepancy of glial support might indirectly intervene neuronal surviving in the presence of TMP, retaining of the neuronal specific MAP-2 protein in neuronal soma by TMP appeared to increase specifically the resistance of neurons to attacks.

Moreover, in the present study we found that TMP retained rattin in association with an increased cell survival in rat retinal cells following either long-term cultivation or H_2O_2 exposures. Exogenous rattin analog, humanin peptide, efficiently rescued cells from lethal exposures to H_2O_2. Studies have shown that humanin protects neuronal cells from damage caused by Alzheimer's insults (Hashimoto et al., 2001; Caricasole et al., 2002). Conversely, downregulation of humanin sensitizes cells to Bax and increases Bax translocation to membranes and promotes the release of cytochrome c for progression of programmed cell death (Guo et al., 2003). TMP treatment significantly attenuated cytochrome c release and activation of caspases in ischemic brain or PC12 cells exposed to H_2O_2 (Cheng et al., 2006; Kao et al., 2006). Thus, our findings support the idea that TMP preserves expression of humanin/rattin to contribute to its mitoprotective effects and to promote, in part, retinal cell survival against attacks, although further studies are warranted to explore the mechanism of TMP-mediated preservation of rattin expression. Moreover, application of exogenous humanin peptide might be an efficient therapeutic approach to counteract cell loss in certain retinopathies.

In summary, we have shown that TMP efficiently protects both neuronal and non-neuronal cell survival in mixed retinal cell cultures against stresses. In addition to its strong antioxidant potency, TMP preserves expression or abundance of both MAP-2 and humanin/rattin that is associated with retinal cell survival. These observations suggest that TMP might be a potential candidate for the development of neuroprotective therapeutics against the loss of retinal cells in optic neuropathies. Exogenous humanin peptide rescues retinal cells and may be a potential therapeutic strategy for certain retinopathies with cell death. Further studies are required to clarify the possible discrepancy of TMP effects on retina between rodents and humans.

Acknowledgements

This study was sponsored by the Fok Ying Tung Education Foundation (Grant No.: 6041) to Q.Z., the National Natural Science Foundation of China (Grant Nos.: 30672275 and 30500555) to J.G., and NIH AG-26637 to Z.T.

References

Bahr M. Live or let die - retinal ganglion cell death and survival during development and in the lesioned adult CNS. Trends Neurosci 2000;23:483–490. [PubMed: 11006465]

Barnham KJ, Masters CL, Bush AI. Neurodegenerative diseases and oxidative stress. Nat Rev Drug Discov 2004;3:205–214. [PubMed: 15031734]

Beatty S, Koh H, Phil M, Henson D, Boulton M. The role of oxidative stress in the pathogenesis of age-related macular degeneration. Surv Ophthalmol 2000;45:115–134. [PubMed: 11033038]

Brewer GJ, Torricelli JR, Evege EK, Price PJ. Optimized survival of hippocampal neurons in B27-supplemented Neurobasal, a new serum-free medium combination. J Neurosci Res 1993;35:567–576. [PubMed: 8377226]

Cai J, Nelson KC, Wu M, Sternberg P Jr. Jones DP. Oxidative damage and protection of the RPE. Prog Retin Eye Res 2000;19:205–221. [PubMed: 10674708]

Caricasole A, Bruno V, Cappuccio I, Melchiorri D, Copani A, Nicoletti F. A novel rat gene encoding a Humanin-like peptide endowed with broad neuroprotective activity. Faseb J 2002;16:1331–1333. [PubMed: 12154011]

Casetta I, Govoni V, Granieri E. Oxidative stress, antioxidants and neurodegenerative diseases. Curr Pharm Des 2005;11:2033–2052. [PubMed: 15974957]

Cheng XR, Zhang L, Hu JJ, Sun L, Du GH. Neuroprotective effects of tetramethylpyrazine on hydrogen peroxide-induced apoptosis in PC12 cells. Cell Biol Int. 2006

Dehmelt L, Halpain S. Actin and microtubules in neurite initiation: are MAPs the missing link? J Neurobiol 2004;58:18–33. [PubMed: 14598367]

Dehmelt L, Halpain S. The MAP2/Tau family of microtubule-associated proteins. Genome Biol 2005;6:204. [PubMed: 15642108]

Fan LH, Wang KZ, Cheng B, Wang CS, Dang XQ. Anti-apoptotic and neuroprotective effects of Tetramethylpyrazine following spinal cord ischemia in rabbits. BMC Neurosci 2006;7:48. [PubMed: 16774675]

Farkas RH, Grosskreutz CL. Apoptosis, neuroprotection, and retinal ganglion cell death: an overview. Int Ophthalmol Clin 2001;41:111–130. [PubMed: 11198138]

Ferreira IL, Duarte CB, Neves AR, Carvalho AP. Culture medium components modulate retina cell damage induced by glutamate, kainate or “chemical ischemia”. Neurochem Int 1998;32:387–396. [PubMed: 9596563]

Fifre A, Sponne I, Koziel V, Kriem B, Yen Potin FT, Bihain BE, Olivier JL, Oster T, Pillot T. Microtubule-associated protein MAP1A, MAP1B, and MAP2 proteolysis during soluble amyloid beta-peptide-induced neuronal apoptosis. Synergistic involvement of calpain and caspase-3. J Biol Chem 2006;281:229–240. [PubMed: 16234245]

Fontaine-Lenoir V, Chambraud B, Fellous A, David S, Duchossoy Y, Baulieu EE, Robel P. Microtubule-associated protein 2 (MAP2) is a neurosteroid receptor. Proc Natl Acad Sci U S A 2006;103:4711–4716. [PubMed: 16537405]

Ge JY, Zhang ZL. [Progress in pharmacology and clinical application of Ligusticum wallichii]. Zhongguo Zhong Xi Yi Jie He Za Zhi 1994;14:638–640. [PubMed: 7719100]

Guo B, Zhai D, Cabezas E, Welsh K, Nouraini S, Satterthwait AC, Reed JC. Humanin peptide suppresses apoptosis by interfering with Bax activation. Nature 2003;423:456–461. [PubMed: 12732850]

Guo L, Salt TE, Maass A, Luong V, Moss SE, Fitzke FW, Cordeiro MF. Assessment of neuroprotective effects of glutamate modulation on glaucoma-related retinal ganglion cell apoptosis in vivo. Invest Ophthalmol Vis Sci 2006;47:626–633. [PubMed: 16431960]

Hashimoto Y, Niikura T, Tajima H, Yasukawa T, Sudo H, Ito Y, Kita Y, Kawasumi M, Kouyama K, Doyu M, Sobue G, Koide T, Tsuji S, Lang J, Kurokawa K, Nishimoto I. A rescue factor abolishing

neuronal cell death by a wide spectrum of familial Alzheimer's disease genes and Abeta. Proc Natl Acad Sci U S A 2001;98:6336–6341. [PubMed: 11371646]

Kao TK, Ou YC, Kuo JS, Chen WY, Liao SL, Wu CW, Chen CJ, Ling NN, Zhang YH, Peng WH. Neuroprotection by tetramethylpyrazine against ischemic brain injury in rats. Neurochem Int 2006;48:166–176. [PubMed: 16316708]

Kapin MA, Doshi R, Scatton B, DeSantis LM, Chandler ML. Neuroprotective effects of eliprodil in retinal excitotoxicity and ischemia. Invest Ophthalmol Vis Sci 1999;40:1177–1182. [PubMed: 10235551]

Krichevsky AM, Kosik KS. RNAi functions in cultured mammalian neurons. Proc Natl Acad Sci U S A 2002;99:11926–11929. [PubMed: 12192088]

Kroemer G, Reed JC. Mitochondrial control of cell death. Nat Med 2000;6:513–519. [PubMed: 10802706]

Levin LA. Mechanisms of optic neuropathy. Curr Opin Ophthalmol 1997;8:9–15. [PubMed: 10176111]

Li X, Yang L, Kang F, Zhang S, Li G, Han Y, Zhai Y. [The protective effect of ligustrazine on optic nerve axons in rabbit eyes with continuous elevated IOP]. Zhonghua Yan Ke Za Zhi 2000;36:442–444. [PubMed: 11853645]429

Li Y, Schlamp CL, Nickells RW. Experimental induction of retinal ganglion cell death in adult mice. Invest Ophthalmol Vis Sci 1999;40:1004–1008. [PubMed: 10102300]

Liao SL, Kao TK, Chen WY, Lin YS, Chen SY, Raung SL, Wu CW, Lu HC, Chen CJ. Tetramethylpyrazine reduces ischemic brain injury in rats. Neurosci Lett 2004;372:40–45. [PubMed: 15531085]

Lin MT, Beal MF. Mitochondrial dysfunction and oxidative stress in neurodegenerative diseases. Nature 2006;443:787–795. [PubMed: 17051205]

Luo X, Heidinger V, Picaud S, Lambrou G, Dreyfus H, Sahel J, Hicks D. Selective excitotoxic degeneration of adult pig retinal ganglion cells in vitro. Invest Ophthalmol Vis Sci 2001;42:1096–1106. [PubMed: 11274091]

Ni JW, Matsumoto K, Watanabe H. Tetramethylpyrazine improves spatial cognitive impairment induced by permanent occlusion of bilateral common carotid arteries or scopolamine in rats. Jpn J Pharmacol 1995;67:137–141. [PubMed: 7616688]

Nishimoto I, Matsuoka M, niikura T. Unravelling the role of Humanin. Trends Mol Med 2004;10:102–105. [PubMed: 15106598]

Pang PK, Shan JJ, Chiu KW. Tetramethylpyrazine, a calcium antagonist. Planta Med 1996;62:431–435. [PubMed: 8923809]

Parone P, Priault M, James D, Nothwehr SF, Martinou JC. Apoptosis: bombarding the mitochondria. Essays Biochem 2003;39:41–51. [PubMed: 14585073]

Richer S. Antioxidants and the eye. Int Ophthalmol Clin 2000;40:1–16. [PubMed: 11064854]

Shih YH, Wu SL, Chiou WF, Ku HH, Ko TL, Fu YS. Protective effects of tetramethylpyrazine on kainate-induced excitotoxicity in hippocampal culture. Neuroreport 2002;13:515–519. [PubMed: 11930173]

Tan Z, Sun X, Hou FS, Oh HW, Hilgenberg LG, Hol EM, van Leeuwen FW, Smith MA, O'Dowd DK, Schreiber SS. Mutant ubiquitin found in Alzheimer's disease causes neuritic beading of mitochondria in association with neuronal degeneration. Cell Death Differ 2007;14:1721–1732. [PubMed: 17571083]

Tan Z, Tu W, Schreiber SS. Downregulation of free ubiquitin: a novel mechanism of p53 stabilization and neuronal cell death. Brain Res Mol Brain Res 2001;91:179–188. [PubMed: 11457508]

Tezel G. Oxidative stress in glaucomatous neurodegeneration: mechanisms and consequences. Prog Retin Eye Res 2006;25:490–513. [PubMed: 16962364]

Wang Y, Chang CF, Morales M, Chou J, Chen HL, Chiang YH, Lin SZ, Cadet JL, Deng X, Wang JY, Chen SY, Kaplan PL, Hoffer BJ. Bone morphogenetic protein-6 reduces ischemia-induced brain damage in rats. Stroke 2001;32:2170–2178. [PubMed: 11546913]

Xu H, Shi DZ, Guan CY. [Clinical application and pharmacological actions of ligustrazine]. Zhongguo Zhong Xi Yi Jie He Za Zhi 2003;23:376–379. [PubMed: 12800423]

Yang JN, Chen JM, Luo L, Lin SC, Li D, Hu SX. Tetramethylpyrazine protected photoreceptor cells of rats by modulating nuclear translocation of NF-kappaB. Acta Pharmacol Sin 2005;26:887–892. [PubMed: 15960898]

Zhang C, Wang SZ, Zuo PP, Cui X, Cai J. Protective effect of tetramethylpyrazine on learning and memory function in D-galactose-lesioned mice. Chin Med Sci J 2004;19:180–184. [PubMed: 15506643]

Zhang Z, Wei T, Hou J, Li G, Yu S, Xin W. Iron-induced oxidative damage and apoptosis in cerebellar granule cells: attenuation by tetramethylpyrazine and ferulic acid. Eur J Pharmacol 2003;467:41–47. [PubMed: 12706453]

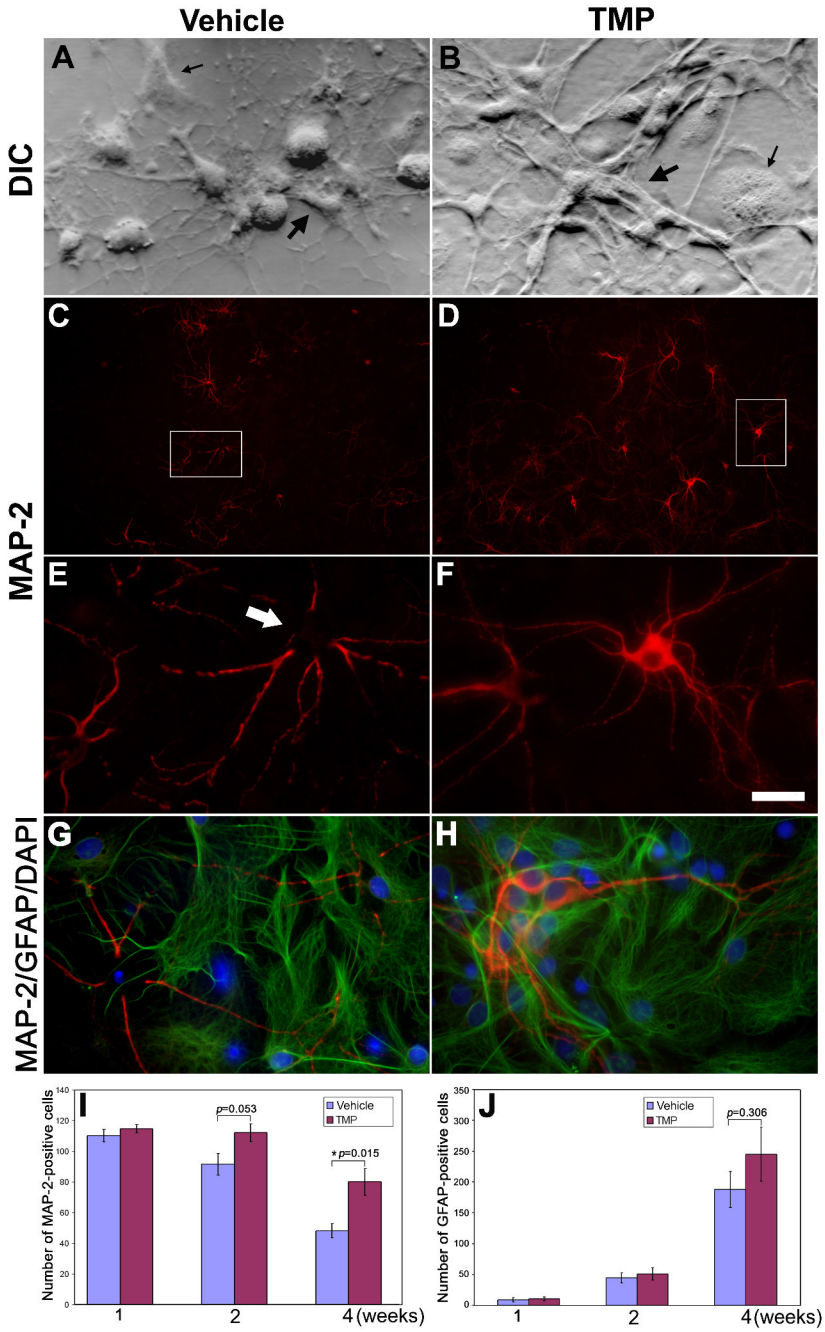

Fig. 1. TMP promotes neuronal survival in mixed retinal cell cultures

(A & B) DIC microscopy shows cell morphology of mixed retinal cell cultures in which the media contained vehicle (A) or 50 μM TMP (B) after 4-week in vitro cultivation. Both neuronal (bold arrow) and non-neuronal (thin arrow) -looking cells are seen in the cultures. Note: retraction of neuronal processes and shrinkage of cell soma are seen in (A). **(C-F)** Immunocytochemistry of MAP-2 reveals MAP-2-positive neurons in retinal cell cultures with either vehicle (C) or TMP (D). High magnification of the insets in (C) and (D) are shown in (E) and (F), respectively. Relatively strong staining of MAP-2 in cell soma is seen in TMP-treated cultures (E) compared to vehicle control. **(G-H)** Fluorescence microscopy of dual immunostaining of MAP-2 and GFAP demonstrates both MAP-2-positive neurons and GFAP-

positive astrocytes in both control and TMP-treated cultures. Nuclei were stained as blue by DAPI. Quantification of MAP-2-positive neurons **(I)** and GFAP-positive astrocytes **(J)** demonstrates significantly higher numbers of survival neurons (p=0.015, N=4) and a slight increase in the number of GFAP-positive astrocytes (p=0.306, N=4) in TMP-treated cultures than vehicle control after 4-week growing in vitro. Bars depict mean ± S.E.M.. Scale bar represents 200 μm in C and D and 20 μm in the other panels.

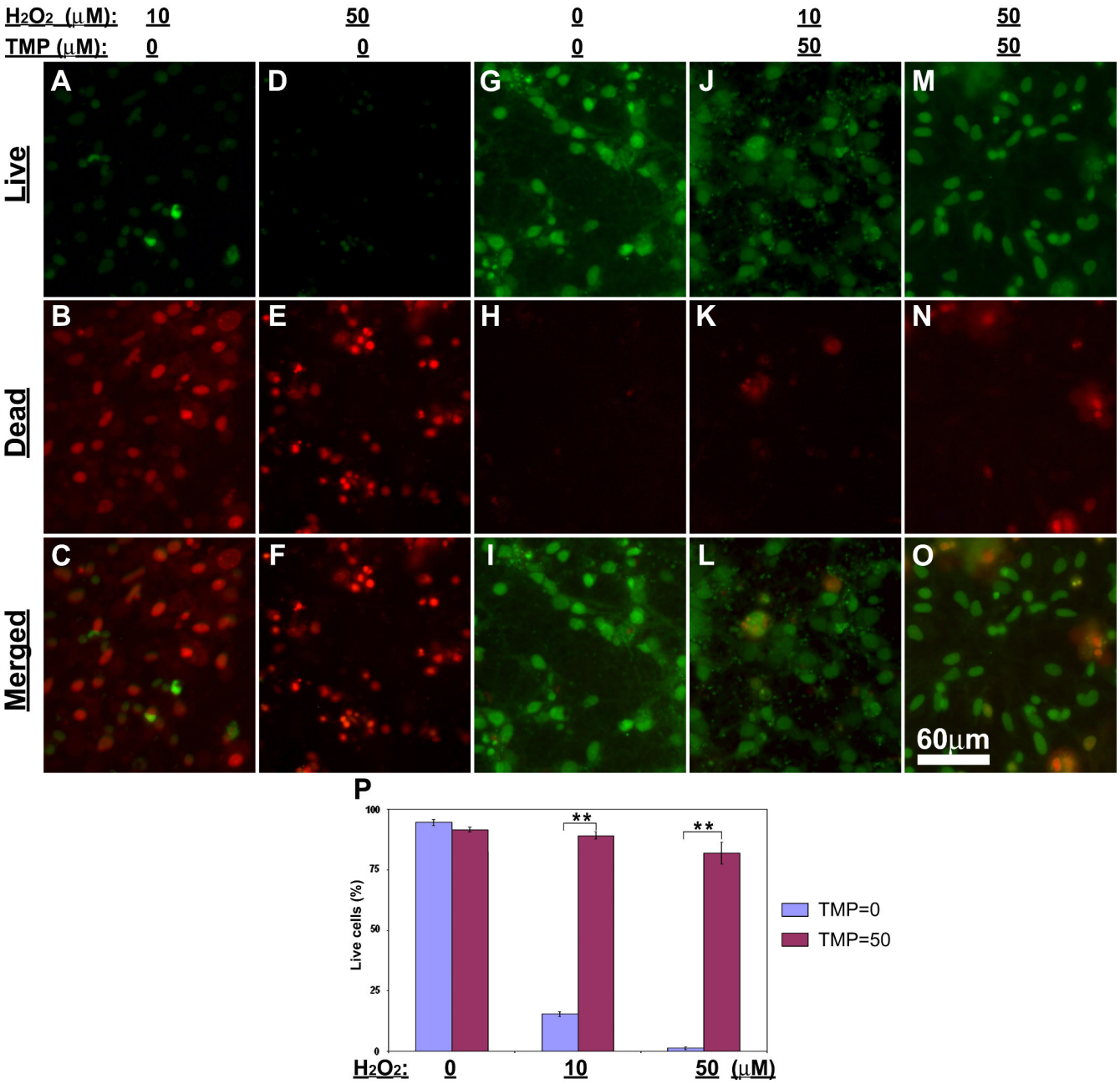

Fig. 2. TMP attenuates hydrogen peroxide-induced cell death in mixed retinal cell cultures

Retinal cell cultures were treated as indicated at the top of the figure. **(A-O)** Fluorescence microcopy following Live-dead cell assay shows live cells (green, A, D, G, J & M), dead cells (red, B, E, H, K & N) and merged images (C, F, I, L & O). **(P)** Quantification of the results shows significantly higher numbers of live cells in vehicle control (H_2O_2 = 0; TMP = 0) as well as hydrogen peroxide-treated cultures with TMP (H_2O_2 = 10 or 50; TMP = 50) than those hydrogen peroxide-treated cultures with the absence of TMP (H_2O_2 = 10 or 50; TMP = 0). Bars depict mean ± S.E.M., $^{**}p < 0.001$ (N = 5).

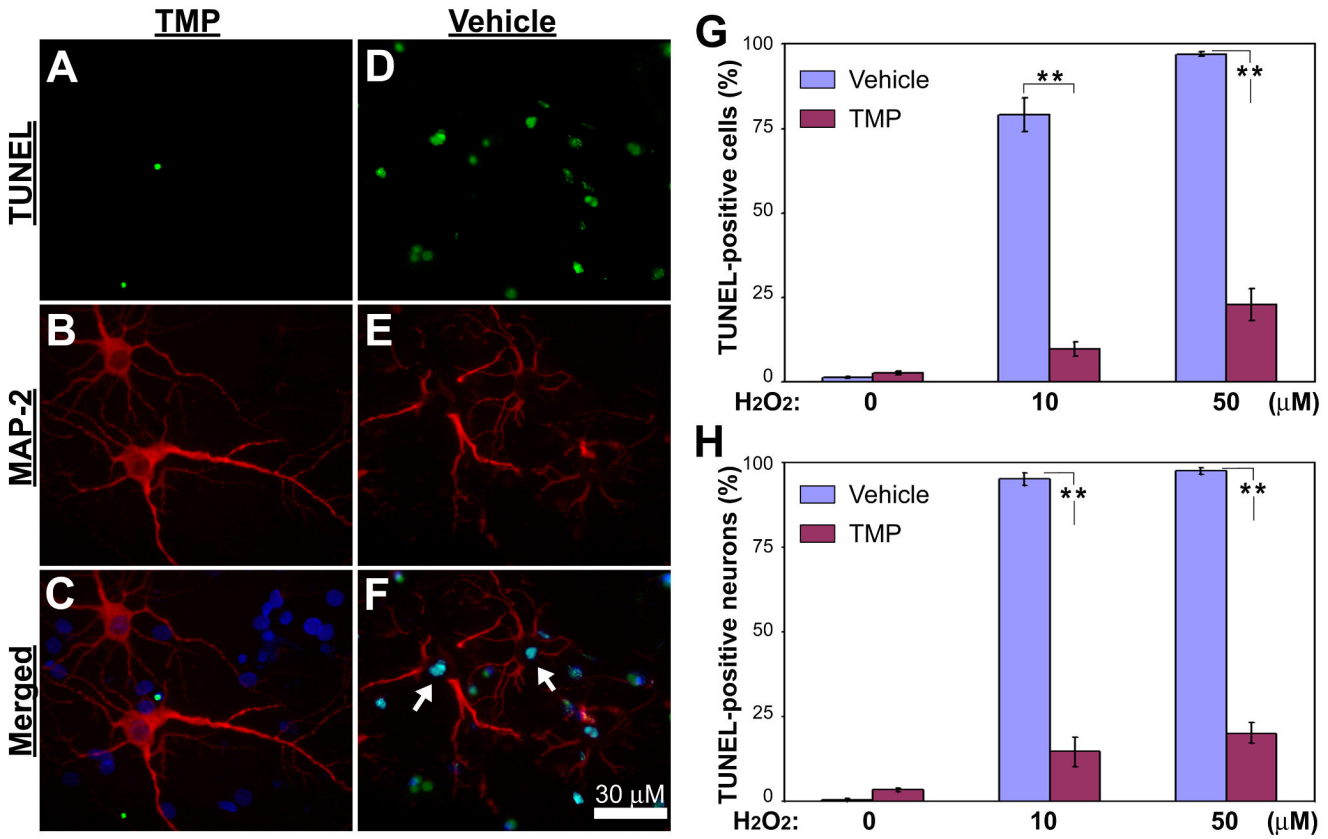

Fig. 3. TUNEL staining of retinal cell cultures after hydrogen peroxide and TMP treatments

(A-F) Retinal cell cultures were treated with 10 μM hydrogen peroxide combined with either 50 μM TMP (A-C) or vehicle (D-F) and examined by fluorescence microscopy following dual staining of TUNEL (green, A & D) and MAP-2 immunoreactivity (red, B & E). Nuclei are shown as blue by DAPI in the merged images (C & F). Note: Several MAP-2-positive neurons (red) in the field from hydrogen peroxide-treated cultures with vehicle are TUNEL-positive (arrows) as shown in merged image (F); In contrast, two MAP-2-positive neurons (red) in the field from cultures treated with both hydrogen peroxide and 50 μM TMP are TUNEL-negative (B & C). **(G & H)** Cells were treated with varying concentrations of H_2O_2 as indicated at the bottom of charts combined with either 50 μM TMP or vehicle. Quantification of TUNEL and DAPI dual staining results shows the percentages of TUNEL-positive cells over total numbers of DAPI-stained nuclei (G); quantification of TUNEL and MAP-2 double-stained cells relative to the numbers of all MAP-2-positive neurons shows significantly lower numbers of damaged MAP-2-positive neurons in the cultures with TMP than those with vehicle (H). The ratios [TUNEL(+)/DAPI(+), i.e., total number of cells; TUNEL(+)-MAP-2-(+)/MAP-2-(+), i.e., total number of MAP-2-(+) neurons] plotted as a function of H_2O_2 concentration. Bars depict mean ± S.E.M., $^{**}p < 0.001$ (N = 4).

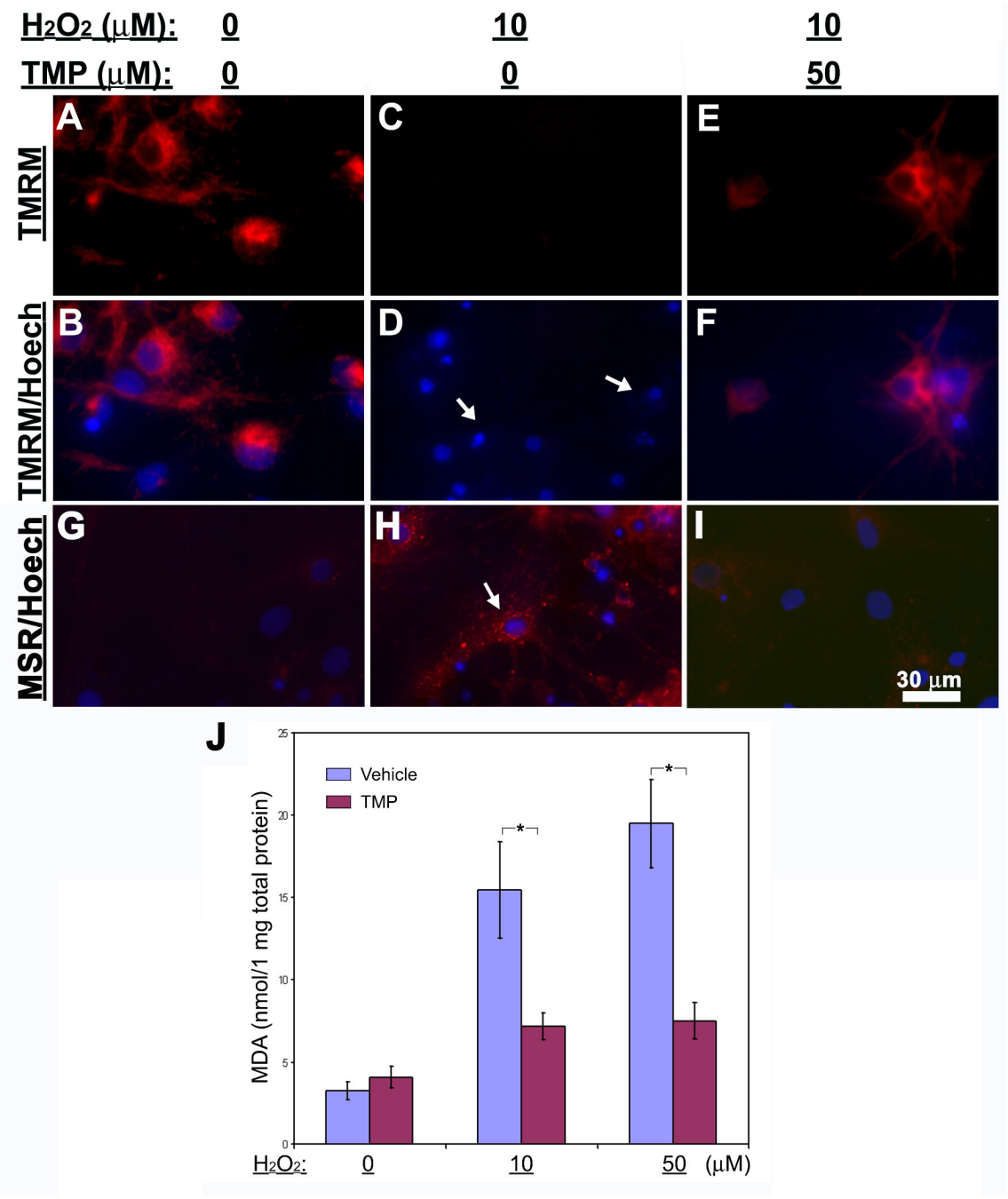

Fig. 4. Inhibition of mitochondrial membrane depolarization, ROS production and lipid peroxidation by TMP

Retinal cell cultures were treated as indicated at the top of the figure. **(A-F)** Fluorescence microscopy reveals that TMRM (red) stains the majority of cells in control (A & B) as well as in hydrogen peroxide-treated group with 50 μM TMP (E & F). Remarkable loss of TMRM staining is detected in the cultures treated with hydrogen peroxide and vehicle (arrows in D). **(G-I)** Fluorescence microscopy demonstrates mitochondrial superoxides in control (G), H_2O_2- (H) and (H_2O_2+TMP)-treated cultures following MitoSox Red (MSR) staining (red). The arrow in (H) indicates positive staining for superoxides. Cell nuclei are shown as blue by Hoechst 33342 (Hoech). **(J)** Formation of malondiadehyde in retinal cell cultures was

measured as a marker for lipid peroxidation resulting from oxidative damage after treatments as indicated. The results are depicted as mean ± S.E.M. *$p < 0.05$ (N = 5).

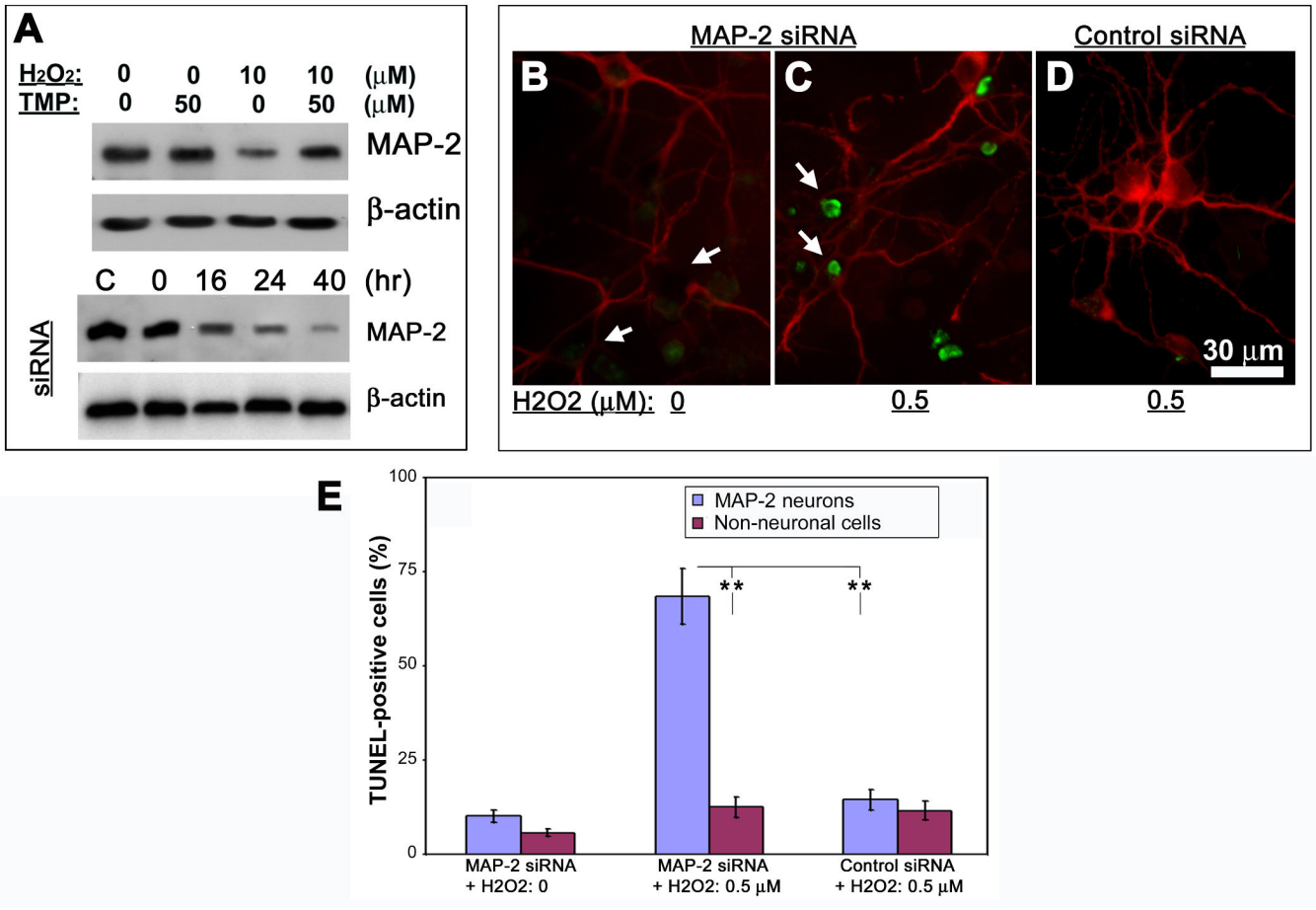

Fig. 5. Prevention of MAP-2 loss by TMP in association with neuronal resistance to ROS stress

(A) Cells were treated as indicated on the top of the first two panels. Western blots show decreased abundance of MAP-2 protein in H_2O_2-treated cells, which is prevented by addition of TMP (first panel). In the separate experiments, whole-cell lysates were prepared from cells transfected with 100 pmol MAP-2 siRNA and Western blotting was performed to show the levels of MAP-2 at indicated times (on the top of third panel). C = control, which was from cells 40 hr after control siRNA transfection. β-actin was used as loading controls. **(B-D)** Cells were transfected with MAP-2 or control siRNA and treated as indicated on the bottom of the panels at 16 hr following transfection. Double-labeling of MAP-2 (red) and TUNEL (green) shows the loss of MAP-2 immunoreactivity in neuronal soma due to siRNA transfection but lack of TUNEL signal in cells without other treatments (arrows in B); TUNEL-positive cells are detected in MAP-2 siRNA-transfected cells 24 hr after exposure to 0.5 μM H_2O_2 (arrows in C); Control siRNA shows no effects on MAP-2 immunoreactivity nor TUNEL signal in cells following 24 hr exposure to 0.5 μM H_2O_2 (D). **(E)** The number of TUNEL-positives cells relative to either MAP-2-labeled neurons, of which part of them had very low MAP-2 signal in neuronal soma, or fully MAP-2-negative non-neuronal cells following the treatments as indicated on the bottom of the chart. Bars depict mean ± S.E.M., $^{**}p < 0.01$ (N = 4).

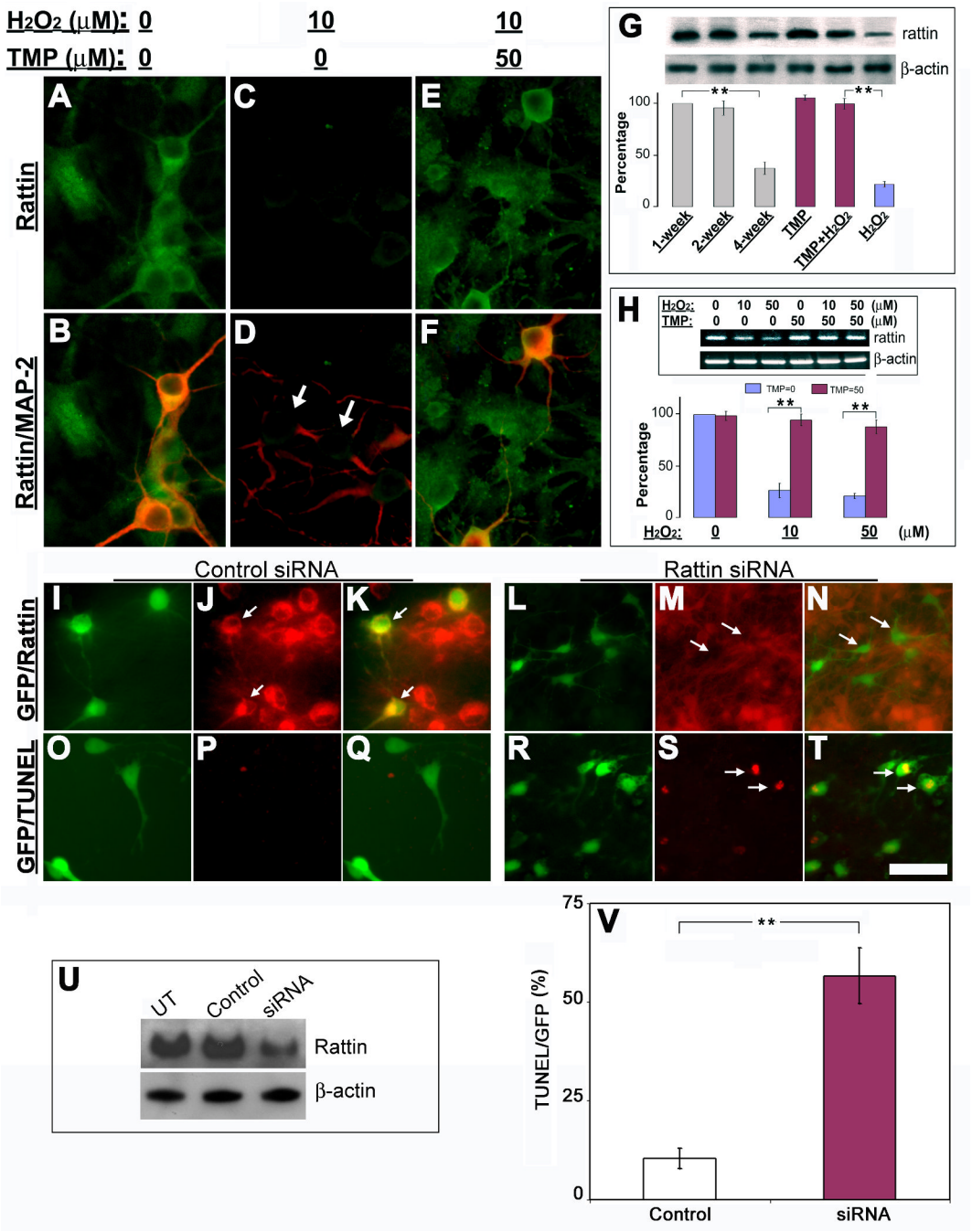

Fig. 6. TMP inhibits ROS-induced downregulation of rattin to promote retinal cell survival

(A-F) Cytoplasmic immunoreactivity of rattin (green) in both MAP-2-positive neurons (red) and other non-neuronal cells in retinal cell cultures treated with vehicles (A & B), 10 μM H_2O_2 alone (C & D), or "10 μM H_2O_2+50 μM TMP" (E & F). Arrows in merged image D indicate rattin-negative neurons. **(G)** Changes in abundance of rattin protein with cultivation time or indicated treatments by Western blots. The results were quantified by optical densitometry and are depicted relative to the 1-week old controls. **(H)** Expression of rattin mRNA in cultures following indicated treatments was examined by RT-PCR. The results are depicted relative to levels in vehicle-treated cells (H_2O_2 = 0; TMP = 0). **(I-T)** siRNA mediated downregulation of rattin associated with retinal cell death visualized by fluorescence

microscopy. Cells were co-transfected with both pEGFP-C3 and either the control siRNA (I-K, O-Q) or rattin siRNA (L-N, R-T). Immunocytochemistry shows that most GFP-positive cells are rattin-immunoreactive in controls (J-K, arrows) but demonstrate remarkably decreased immunoreactivity of rattin in cells 30 hr after rattin siRNA transfection (L-N, arrows). TUNEL staining (red) demonstrates no evident cell death in control (O-Q) and extensive cell damage in most GFP-positive cells (R-T, arrows). **(U)** Abundance of rattin in cells 30 hr after transfection by Western blots. UT = untransfected. **(V)** Quantification of TUNEL-positive cells in cells 30 hr after transfection. β-actin was used as loading controls. Bars depict mean ± S.E.M., $^{**}p < 0.01$ (N = 4). Scale bar = 30 μm in A-F, 40 μm in I-T.

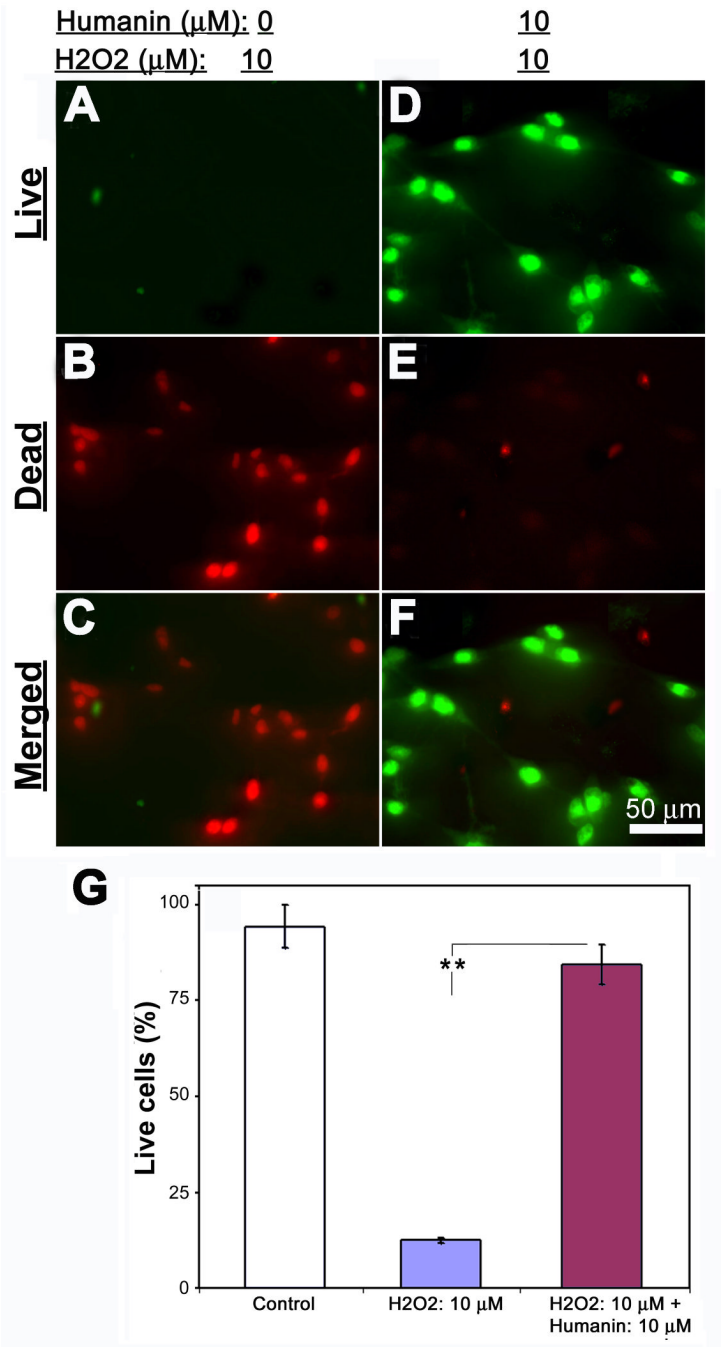

Fig. 7. Exogenous humanin peptide protects retinal cell from ROS-induced cell death

Retinal cell cultures were treated as indicated at the top of the figure. **(A-F)** Fluorescence microcopy following Live-dead cell assay demonstrates live cells (green, A & D), dead cells (red, B & E) and merged images (C & F). **(G)** Quantification of the results shows significantly higher numbers of live cells in vehicle control as well as hydrogen peroxide-treated cultures with humanin (H_2O_2 = 10 μM; humanin = 10 μM) than those cultures treated with hydrogen peroxide alone (H_2O_2 = 10 μM). Bars depict mean ± S.E.M., $^{**}p < 0.001$ (N = 5).